Chemical Physics 441 (2014) 66–76

Contents lists available at ScienceDirect

Chemical Physics

journal homepage: www.elsevier.com/locate/chemphys

State-to-state description of reacting air flows behind shock waves

O.V. Kunova *, E.A. Nagnibeda

Department of Mathematics and Mechanics, Saint Petersburg State University, 28, Universitetski pr., Saint Petersburg 198504, Russia

ARTICLE INFO

Article history:
Received 10 May 2014
In final form 5 July 2014
Available online 12 July 2014

Keywords:
Shock wave
Air mixture
Non-equilibrium vibrational and chemical kinetics
State-to-state approach

ABSTRACT

In the present paper, non-equilibrium flows of the 5-component air mixture $N_2(i)/O_2(i)/NO(i)/N/O$ behind shock waves are studied taking into account the state-to-state vibrational and chemical kinetics. Equations for the non-equilibrium kinetics including vibrational energy transitions, dissociation, recombination and Zeldovich reactions of NO formation are coupled to gas dynamic equations and solved numerically for different test cases of the re-entry conditions into the Earth atmosphere. Peculiarities of air parameters behind a shock wave formed in an initially vibrationally excited mixture are studied. Various models for state-dependent rates of kinetic processes are used for calculations and their applicability for prediction of flow parameters is discussed. The results obtained in the state-to-state approach are compared with those based on multi-temperature and one-temperature vibrational distributions and estimations for an accuracy of the simplified models are presented.

1. Introduction

Investigations of the non-equilibrium chemical kinetics and internal energy relaxation are important for the flows behind the shock waves appearing near hypersonic space bodies, in nozzles and jets, in high enthalpy facilities, combustion and technology processes. A large part of descending trajectory of space vehicles in their re-entry into the Earth atmosphere lies at high altitudes of about 50–70 km where characteristic times of kinetic and gas dynamic processes become comparable. Then, non-equilibrium excitation of internal degrees of freedom and chemical reactions should be taken into account in the gas flow studies. The experimental research of high-temperature flows of multi-component reacting mixtures meets serious difficulties because the conditions of strong deviations from the equilibrium are not completely simulated in present aerodynamic facilities. Therefore elaboration of theoretical and numerical models for non-equilibrium gas flows providing of satisfactory accuracy and at the same time suitable for applications, is a vital problem of the up-to-date physical–chemical aerodynamics.

Fundamental kinetic theory for non-equilibrium reacting gas mixtures [1–3] provides various approaches for description of multi-component flows at different deviations from thermal and chemical equilibrium. The most accurate models require joint consideration of the equations for gas dynamic parameters and state-to-state non-equilibrium kinetics of internal energy relaxation and chemical reactions.

The most detailed study of roto-vibrational relaxation in molecular gases is based on master equations for distributions over rotational and vibrational energies with the use of state dependent transition rate coefficients. In recent time a substantial advancement in the numerical solution of these equations has been reached including calculations of collisional cross sections and roto-vibrational transition probabilities [4–11]. The interesting coarse grain model has very recently been derived from detailed ro-vibrational state-to-state models in [12]. However, the use of the accurate data obtained within this approach for aerodynamic problems is hardly possible because it requires to consider tens of thousands of state-to-state energy transitions and chemical reactions. Moreover, the data are still obtained mainly for (N_2, N) and (O_2, O) mixtures and for limited temperature ranges.

Experimental data show that under wide conditions in high-temperature gases excluding light molecules like hydrogen, translational and rotational degrees of freedom equilibrate much faster compared to vibrational and chemical relaxation [13–15]. Therefore the vibrational and chemical non-equilibrium kinetics in the air components is often studied allowing the assumption about equilibrium or weakly non-equilibrium distributions over velocities and rotational energies. In this case gas dynamic equations in the Euler or Navier–Stokes approximations are coupled to the equations for vibrational level populations of different chemical species and atomic concentrations. This approach received much attention during two last decades for numerical simulations of different flows of air components such as near re-entering bodies

* Corresponding author.
E-mail addresses: kunova.olga@gmail.com (O.V. Kunova), e_nagnibeda@mail.ru (E.A. Nagnibeda).

http://dx.doi.org/10.1016/j.chemphys.2014.07.007
0301-0104/

[16,17], behind shock waves [18–20], in nozzles [21–25], in a boundary layer [26,27] and in a shock layer near re-entering bodies [28], in a shock tunnel nozzle and behind a shock wave in its test section [29]. However, in the majority of papers only two-component mixtures are considered in the state-to-state flow simulations taking into account vibration–dissociation coupling.

The state-to-state description of multi-component mixtures requires a solution of a large number of equations for internal energy level populations of different chemical species and an input into computational codes a lot of analytical expressions for state-dependent rate coefficients of kinetic processes. In the case of multi-component mixtures one should include to a kinetic scheme not only internal energy transitions, dissociation and recombination processes but also exchange chemical reactions with rate coefficients dependent, in a general case, on internal energy levels of reagents and products. It is obvious that an accuracy of data on reaction rate coefficients and estimation of their influence on gas flow parameters are extremely important for a reliable prediction of gas flow parameters.

In this paper the flows of the shock heated five-component air mixture are studied taking into account non-equilibrium state-to-state vibration and chemical kinetics. The closed set of equations for gas dynamic parameters, number densities of atoms and molecular vibrational distributions is solved numerically for Mach numbers $M = 10,\ 15$ and the following effects are considered. First, the influence of free stream conditions and anharmonicity of molecular vibrations on the gas temperature, mixture composition and vibrational level populations in the relaxation zone behind the shock is studied. Two test cases of both equilibrium and vibrationally excited flow before the shock front are considered and peculiarities of air parameters behind the shock wave occurring in a vibrationally excited flow are shown. The effect of vibrational excitation in the free stream on the relaxation zone structure for the reacting air mixture has not been studied before. Secondly, for better understanding of the impact of models for rates of non-equilibrium processes on air flow parameters in the relaxation zone, various analytical expressions for state-dependent rate coefficients for exchange reactions available in the literature (see [14] and references therein) are incorporated into the numerical code and the comparison of the data obtained using different models is discussed. This important effect was studied before by some authors for vibrational energy transitions [30] and dissociation of air species [31] but for exchange reactions it is not still considered.

And thirdly, the results obtained on the basis of the state-to-state approximation are compared with those found for the same conditions using two-temperature [32] and one-temperature vibrational distributions and the impact of the vibrational non-equilibrium on chemical reactions and air flow parameters is shown.

2. Governing equations

It is known from experimental data [13,14] that in high-temperature flows relaxation times for different kinetic processes satisfy the following relations:

$$\tau_{el} \lesssim \tau_{rot} \ll \tau_{vibr} < \tau_{react} \sim \Theta. \tag{1}$$

Here $\tau_{el},\ \tau_{rot},\ \tau_{vibr},\ \tau_{react}$ are the relaxation times for translational, rotational, vibrational degrees of freedom and chemical reactions, respectively, Θ is the mean time of gas dynamic parameters variation.

Rapid air compression within a thin shock front with the length of about several mean free paths results in a temperature jump and fast translational–rotational relaxation. Due to a substantial difference between relaxation times, the equilibrium or weakly non-equilibrium distributions over translation and rotational energies establish and then maintain in the relaxation zone where excitation of vibrational degrees of freedom and chemical reactions proceed in a strongly non-equilibrium regime along with macroscopic parameters changing. The length of relaxation zone reaches many tens or even hundreds mean free paths.

The complete scheme of the non-equilibrium kinetic processes in the mixture $N_2(i)$, $O_2(i)$, $NO(i)$, N, O in a relaxation zone includes: *VV* vibration energy exchanges at the collisions of the same molecular species, *VV′* exchanges between different species and *VT*(*TV*) exchanges between vibrational and translational energies, dissociation and recombination

$$N_2(i) + M \rightleftarrows N + N + M, \tag{2}$$
$$O_2(i) + M \rightleftarrows O + O + M, \tag{3}$$
$$NO(i) + M \rightleftarrows N + O + M, \tag{4}$$

$(M = N_2, O_2, NO, N, O)$

and Zeldovich exchange reactions of NO formation

$$N_2(i) + O \rightleftarrows NO(i') + N, \tag{5}$$
$$O_2(i) + N \rightleftarrows NO(i') + O. \tag{6}$$

In the present paper we do not take into account the processes of electronic excitation, ionization and radiation and therefore the temperature range is restricted by the conditions when the influence of these processes on the parameters behind the shock front remains weaker than that of vibration and chemical relaxation. Simultaneous *TRV* (*VTR*) exchanges of vibrational, rotational and translational energies are neglected in the considered mixture as less probable [14].

Under the condition (1), the set of basic flow parameters for the considered mixture along with the gas temperature $T(\mathbf{r}, t)$, macroscopic gas velocity $\mathbf{v}(\mathbf{r}, t)$ and number densities of atoms $n_N(\mathbf{r}, t)$, $n_O(\mathbf{r}, t)$, includes the populations of different vibrational levels i of molecular species $n_{N_2 i}(\mathbf{r}, t)$, $n_{O_2 i}(\mathbf{r}, t)$, $n_{NOi}(\mathbf{r}, t)$ ($\mathbf{r}$, t are space and time variables). The closed system of equations for these parameters is derived from the kinetic equations for distribution functions in Ref. [3] on the basis of the Chapman–Enskog method generalized for reacting mixtures for the condition (1). In the zero-order approximation for inviscid air flows we obtain:

$$\frac{\partial n_{ci}}{\partial t} + \nabla \cdot (n_{ci}\mathbf{v}) = R_{ci}^{vibr} + R_{ci}^{2\leftrightarrow 2} + R_{ci}^{2\leftrightarrow 3}, \quad i = 0, 1, \ldots l_c, \quad c = N_2, O_2, NO, \tag{7}$$

$$\frac{\partial n_N}{\partial t} + \nabla \cdot (n_N \mathbf{v}) = R_N^{2\leftrightarrow 2} + R_N^{2\leftrightarrow 3}, \tag{8}$$

$$\frac{\partial n_O}{\partial t} + \nabla \cdot (n_O \mathbf{v}) = R_O^{2\leftrightarrow 2} + R_O^{2\leftrightarrow 3}, \tag{9}$$

$$\frac{\partial \mathbf{v}}{\partial t} + (\mathbf{v} \cdot \nabla)\mathbf{v} + \frac{1}{\rho}\nabla p = 0, \tag{10}$$

$$\frac{\partial U}{\partial t} + (\mathbf{v} \cdot \nabla)U + \frac{p}{\rho}\nabla \cdot \mathbf{v} = 0. \tag{11}$$

Here U is the total energy per unit mass presented as a sum of translational, rotational, vibrational and formation energies:

$$\rho U = \frac{3}{2}nkT + (n_{N_2} + n_{O_2} + n_{NO})kT + \sum_{c,i}\varepsilon_i^c n_{ci} + \sum_c \varepsilon_c n_c, \tag{12}$$

where ρ, n are the mass and number mixture densities, k is the Boltzmann constant, ε_i^c is the vibrational energy of a molecule c species at the i-th vibrational level, ε_c is the formation energy of a particle c species, n_c, n_{ci} are the number density and vibrational population of i-th level for species c.

The vibrational energies are simulated using the anharmonic oscillator model, then the numbers l_c of excited vibrational levels of molecules N_2, O_2, NO are taken as $l_{N_2} = 46$, $l_{O_2} = 35$, $l_{NO} = 38$.

Thus, the system (7)–(11) contains 124 equations for state-to-state vibrational-chemical kinetics and two conservation equations for impulse and total energy. Source terms in Eqs. (7)–(9) describe vibrational energy transitions and chemical reactions. In the case of 1-D steady-state flow behind a plane shock wave the equations (7)–(11) for the functions $n_{N_2 i}(x)$, $n_{O_2 i}(x)$, $n_{NOi}(x)$, $n_N(x)$, $n_O(x)$, $T(x)$, $v(x)$ take the form:

$$\frac{d(vn_{N_2 i})}{dx} = R^{vibr}_{N_2 i} + R^{2\leftrightarrow 2}_{N_2 i} + R^{2\leftrightarrow 3}_{N_2 i}, \quad i = 0, 1, \ldots l_{N_2}, \tag{13}$$

$$\frac{d(vn_{O_2 i})}{dx} = R^{vibr}_{O_2 i} + R^{2\leftrightarrow 2}_{O_2 i} + R^{2\leftrightarrow 3}_{O_2 i}, \quad i = 0, 1, \ldots l_{O_2}, \tag{14}$$

$$\frac{d(vn_{NOi})}{dx} = R^{vibr}_{NOi} + R^{2\leftrightarrow 2}_{NOi} + R^{2\leftrightarrow 3}_{NOi}, \quad i = 0, 1, \ldots l_{NO}, \tag{15}$$

$$\frac{d(vn_N)}{dx} = R^{2\leftrightarrow 2}_N + R^{2\leftrightarrow 3}_N, \tag{16}$$

$$\frac{d(vn_O)}{dx} = R^{2\leftrightarrow 2}_O + R^{2\leftrightarrow 3}_O, \tag{17}$$

$$\rho_0 v_0^2 + p_0 = \rho v^2 + p, \tag{18}$$

$$h_0 + \frac{v_0^2}{2} = h + \frac{v^2}{2}. \tag{19}$$

Here $p = nkT$ is the pressure, subscript "0" indicates the values of parameters in the free stream, h is the enthalpy of the mixture per unit mass:

$$h = \sum_c h_c Y_c, \tag{20}$$

$Y_c = \rho_c/\rho$ are the mass fractions of molecules and atoms,

$$h_c = \frac{5}{2}\bar{R}_c T + \frac{\varepsilon_c}{m_c} \quad \text{for} \quad c = N, O,$$

$$h_c = \frac{7}{2}\bar{R}_c T + \frac{1}{\rho_c}\sum \varepsilon_i^c n_{ci} + \frac{\varepsilon_c}{m_c} \quad \text{for} \quad c = N_2, O_2, NO,$$

where $\bar{R}_c$ is the specific gas constant of species c, m_c is a particle mass.

Let us consider the source terms in Eqs. (13)–(17). The terms $R^{2\leftrightarrow 2}_{ci}$ ($c = N_2, O_2, NO$) describe changing of vibrational level populations due to the exchange reactions (5) and (6):

$$R^{2\leftrightarrow 2}_{N_2 i} = \sum_{i'=0}^{l_{NO}} \left(n_{NOi'} n_N k^{N,O}_{NOi',N_2 i} - n_{N_2 i} n_O k^{O,N}_{N_2 i,NOi'} \right), \tag{21}$$

$$R^{2\leftrightarrow 2}_{O_2 i} = \sum_{i'=0}^{l_{NO}} \left(n_{NOi'} n_O k^{O,N}_{NOi',O_2 i} - n_{O_2 i} n_N k^{N,O}_{O_2 i,NOi'} \right), \tag{22}$$

$$R^{2\leftrightarrow 2}_{NOi} = \sum_{i'=0}^{l_{N_2}} \left(n_{N_2 i'} n_{Ok^{O,N}_{N_2 i',NOi}} - n_{NOi} n_{Nk^{N,O}_{NOi,N_2 i'}} \right) + \sum_{i'=0}^{l_{O_2}} \left(n_{O_2 i'} n_{Nk^{N,O}_{O_2 i',NOi}} - n_{NOi} n_{Ok^{O,N}_{NOi,O_2 i'}} \right), \tag{23}$$

where $k^{O,N}_{N_2 i,NOi'}$, $k^{N,O}_{O_2 i,NOi'}$ are the rate coefficients of the forward reactions (5) and (6), the coefficients $k^{N,O}_{NOi',N_2 i}$, $k^{O,N}_{NOi',O_2 i}$ correspond to the backward reactions.

The expressions $R^{2\leftrightarrow 3}_{ci}$ describe dissociation and recombination (2)–(4):

$$R^{2\leftrightarrow 3}_{N_2 i} = \sum_M n_M \left(n_N^2 k^M_{rec,N_2 i} - n_{N_2 i} k^M_{N_2 i,diss} \right), \tag{24}$$

$$R^{2\leftrightarrow 3}_{O_2 i} = \sum_M n_M \left(n_O^2 k^M_{rec,O_2 i} - n_{O_2 i} k^M_{O_2 i,diss} \right), \tag{25}$$

$$R^{2\leftrightarrow 3}_{NOi} = \sum_M n_M \left(n_N n_O k^M_{rec,NOi} - n_{NOi} k^M_{NOi,diss} \right). \tag{26}$$

Here $k^M_{N_2 i,diss}$, $k^M_{O_2 i,diss}$, $k^M_{NOi,diss}$ are the dissociation rate coefficients for the molecules $N_2(i)$, $O_2(i)$ and $NO(i)$ in result of a collision with a particle M = N_2, O_2, NO, N, O, $k^M_{rec,N_2 i}$, $k^M_{rec,O_2 i}$, $k^M_{rec,NOi}$ are the recombination rate coefficients.

The terms $R^{vibr}_{ci} = R^{VT}_{ci} + R^{VV}_{ci} + R^{VV'}_{ci}$ correspond to $VT(TV)$, VV and VV' vibrational energy exchanges:

$$R^{VT}_{ci} = \sum_M \sum_{i'=0}^{l_c} n_M \left(n_{ci'} k^M_{c,i'\to i} - n_{ci} k^M_{c,i\to i'} \right), \quad c = N_2, O_2, NO, \tag{27}$$

$$R^{VV}_{ci} = \sum_{j=0}^{l_c} \sum_{i'=0}^{l_c} \sum_{j'=0}^{l_c} \left(n_{ci'} n_{cj'} k^{c,j'\to j}_{c,i'\to i} - n_{ci} n_{cj} k^{c,j\to j'}_{c,i\to i'} \right), \tag{28}$$

$$R^{VV'}_{ci} = \sum_d \sum_{j=0}^{l_d} \sum_{i'=0}^{l_c} \sum_{j'=0}^{l_d} \left(n_{ci'} n_{dj'} k^{d,j'\to j}_{c,i'\to i} - n_{ci} n_{dj} k^{d,j\to j'}_{c,i\to i'} \right), \tag{29}$$

$$d = N_2, O_2, NO, \quad d \neq c,$$

where $k^M_{c,i\to i'}$, $k^{c,j\to j'}_{c,i\to i'}$ and $k^{d,j\to j'}_{c,i\to i'}$ are the rate coefficients for $VT(TV)$, VV and VV' transitions, respectively, i, i' and j, j' are the vibrational states of molecules before and after a collision.

The terms $R^{2\leftrightarrow 2}_N$, $R^{2\leftrightarrow 3}_N$, $R^{2\leftrightarrow 2}_O$ and $R^{2\leftrightarrow 3}_O$ have the form:

$$R^{2\leftrightarrow 2}_N = -\sum_{i=0}^{l_{N_2}} R^{2\leftrightarrow 2}_{N_2 i} + \sum_{i=0}^{l_{O_2}} R^{2\leftrightarrow 2}_{O_2 i}, \tag{30}$$

$$R^{2\leftrightarrow 3}_N = -2\sum_{i=0}^{l_{N_2}} R^{2\leftrightarrow 3}_{N_2 i} - \sum_{i=0}^{l_{NO}} R^{2\leftrightarrow 3}_{NOi}, \tag{31}$$

$$R^{2\leftrightarrow 2}_O = -\sum_{i=0}^{l_{O_2}} R^{2\leftrightarrow 2}_{O_2 i} + \sum_{i=0}^{l_{N_2}} R^{2\leftrightarrow 2}_{N_2 i}, \tag{32}$$

$$R^{2\leftrightarrow 3}_O = -2\sum_{i=0}^{l_{O_2}} R^{2\leftrightarrow 3}_{O_2 i} - \sum_{i=0}^{l_{NO}} R^{2\leftrightarrow 3}_{NOi}, \tag{33}$$

and define the variation of number densities of atoms.

3. Reaction rate coefficients

The important problem for numerical simulations of multi-component reacting mixtures is the choice of adequate models for the state-dependent rate coefficients of kinetic processes which are involved in source terms of the equations for the detailed vibrational-chemical kinetics. The analysis of available models for vibrational energy transitions and dissociation–recombination processes in air components and their applications for aerodynamic problems is widely presented in the literature (see Refs. in [33,3,34]).

Among frequently used models for vibrational energy transitions we can mention the formulas of the Schwartz, Slawsky and Herzfeld theory [35] (usually called SSH-theory) generalized by Gordiets for anharmonic oscillators [36], as well as semi-classical model of the forced harmonic oscillator (FHO) elaborated by Adamovich et al. [19] and the correction factor introduced by Park [29] to FHO model to reproduce experimental data. Quasi-classical trajectory calculations for vibrational energy transitions and dissociation in (N_2,N) and (O_2,O) systems are carried out in [43–45]. Analytical expressions are proposed by Capitelli et al. [26,37] for interpolation of accurate trajectory calculations of Billing et al. [38,39] for vibrational energy transitions in (N_2,N) and (O_2,O) mixtures. These approximations are convenient for a practical use but

they are given for temperatures lower than 12,000 K and not for all collisions in the considered five-component air mixture.

Therefore in the present paper we used the generalized formulas of SSH-theory for anharmonic oscillators. The comparison of flow parameters for shock heated (N_2,N) mixture obtained using different models for vibrational energy transitions is presented in Refs. [30,3].

For the rate coefficients of dissociation from various vibrational states we used the modification of the Treanor–Marrone model [40] in the state-to-state approach [18,3]:

$$k^{M}_{ci,diss} = Z_{ci}(T)k^{M}_{c,diss-eq}(T), \tag{34}$$

where Z_{ci} is the state-dependent non-equilibrium factor

$$Z_{ci}(T) = Z_{ci}(T,U_c) = \frac{Z^{vibr}_c(T)}{Z^{vibr}_c(-U_c)} \exp\left(\frac{\varepsilon^c_i}{k}\left(\frac{1}{T}+\frac{1}{U_c}\right)\right) \tag{35}$$

and U_c is the parameter of the model (in calculations $U_c = D_c/6k$ is taken), Z^{vibr}_c is the equilibrium vibrational partition function. The thermal equilibrium dissociation rate coefficients $k^{M}_{c,diss-eq}$ are represented by the empirical Arrhenius law:

$$k^{M}_{c,diss-eq}(T) = AT^b \exp\left(-\frac{D_c}{kT}\right), \tag{36}$$

where D_c is the dissociation energy, the coefficients A and b for air components are available in a number of works [33,13,41,42,14].

The comparison of the state-specific N_2 dissociation rate coefficients obtained using the expression (34) for different U_c values for various temperature intervals and accurate quasi-classical trajectory calculations [43] is discussed in [31], whereas the influence of different dissociation models on (N_2,N) mixture parameters behind a shock waves is studied in [30].

Rate coefficients for bimolecular exchange reactions depending on vibrational states of reagents and products have been less thoroughly studied than those for dissociation and energy transitions. The accurate theoretical approach to this problem primarily requires a calculation for the state-dependent differential cross sections for collisions resulting in chemical reactions, and their averaging over velocity distributions. In recent years, the dynamics of atmospheric reactions has been studied and quasi-classical trajectory calculations for the cross sections and the state-dependent rate coefficients for exchange reactions have been carried out by several authors (see [4,5,46,47] and Refs. [33,14,3]). For application of existing numerical results to problems of non-equilibrium gas dynamics, analytical expressions for the rate coefficients dependent on vibrational states of molecules participating in reactions are needed. The analysis of some analytical expressions for particular reactions is given in [33,14].

In the present paper we used four models given in [14] for the rate coefficients k_{fi} of the forward endothermic reactions of NO formation

$$N_2(i) + O \rightarrow NO + N, \tag{37}$$

$$O_2(i) + N \rightarrow NO + O. \tag{38}$$

In the first model proposed by Rusanov and Fridman [48] assuming 100% efficiency of translational energy of reactants in overcoming the activation barrier E_a the state-specific rate coefficients are written in the form

$$k_{fi}(T) = A(T)\exp\left(-\frac{E_a - \alpha\varepsilon^c_i}{kT}\tilde{\Theta}\left(E_a - \alpha\varepsilon^c_i\right)\right), \tag{39}$$

where $\tilde{\Theta}$ is the Heaviside function, α is the vibrational energy efficiency coefficient given in Table 1, $A(T)$ is close to the collision frequency per unit time $A \approx \pi r_0^2(8kT/\pi\bar{\mu})^{1/2}$ (r_0 is the collision diameter, $\bar{\mu}$ is the reduced mass of colliding particles).

The second model is presented by Warnatz et al. [49] on the basis of calculations using the chemical active collision theory [50]:

$$k_{fi}(T) = C(i+1)T^{\beta}\exp\left(-\frac{E_a - \varepsilon^c_i}{kT}\tilde{\Theta}\left(E_a - \varepsilon^c_i\right)\right). \tag{40}$$

The coefficients C, β are given in Table 1.

Next two models for the state-specific rate coefficients approximate numerical solutions of dynamic problems for reactive molecular collisions. In so doing the following expression is given by Polak et al. in [51]

$$k_{fi}(T) = A(T)\exp\left(-\frac{E_a - \alpha\varepsilon^c_i}{\gamma kT}\tilde{\Theta}\left(E_a - \alpha\varepsilon^c_i\right)\right), \tag{41}$$

where the parameters α and γ describe the contribution of the vibrational and translational energies in a reaction and are also given in Table 1.

The following expressions containing several adjusting parameters are suggested by Bose and Candler [4,5] on the basis of quasi-classical trajectory calculations for the reaction $N_2(i) + O \rightarrow NO + N$:

$$\log_{10}k^{O,N}_{N_2 i,NO} = b_0 + b_1\varepsilon^{N_2}_i + b_2\left(\varepsilon^{N_2}_i\right)^2 + b_3\left(\varepsilon^{N_2}_i\right)^3 \tag{42}$$

and for the reaction $O_2(i) + N \rightarrow NO + O$:

$$\log_{10}k^{N,O}_{O_2 i,NO}(T) = \sum_{m,k} a_{m,k}T^m\left(\varepsilon^{O_2}_i\right)^k. \tag{43}$$

The coefficients b_j and $a_{m,k}$ are given in Tables 2 and 3. In Eqs. (39)–(43) the rate coefficients are in $mol^{-1}\,cm^3\,s^{-1}$ and vibrational energy ε^c_i is in eV.

Since the coefficients in Eq. (42) are given only for three temperature values, in calculations we interpolated the polynomial coefficients for needed temperature values.

Figs. 1 and 2 show the variation of the forward reaction rate coefficients k_{fi}, obtained using the expressions (39)–(43) in dependence on the gas temperature for fixed N_2 and O_2 vibrational level $i = 10$. Calculation show that all the models yield rising of the reaction rate coefficients with the gas temperature and vibrational level number. We can notice that for both reactions (37) and (38) the expressions proposed by Rusanov, Fridman and Polak et al. give rather close values of the rate coefficients whereas the use of the models of Warnatz et al. and Bose, Candler for the first reaction provides more pronounced distinctions which reach an order of magnitude. At the same time, the difference in k_{fi} values found using the expressions given by Warnatz et al. and Bose, Candler for the second reaction is found to be small.

For validation of the considered models, the expressions (39)–(43) have been averaged over vibrational energies with the Boltzmann equilibrium distributions with the gas temperature T and then compared with ones found using the empirical Arrhenius expressions for the thermal equilibrium reaction rate coefficients with the parameters given in [52]. Figs. 3 and 4 show that the models of Warnatz et al. (40) and Bose, Candler (42) and (43) lead to the closer agreement of the averaged coefficients with the Arrhenius ones than two other models (39) and (41) for both reactions. Based on this comparison, the models (40) and (42), (43) could be recommended for numerical simulations, however, it is worth to keep in mind that coefficients in the expression (42) are given only for limited temperature interval and can lead to some inaccuracies in the wider temperature conditions.

Rate coefficients of the backward reactions have been calculated using the detailed balance principle [3]. For all models the rate coefficients for reverse reaction (37) are greater than for the

Table 1
The coefficients in Eqs. (39)–(41).

Eq.	$N_2 + O \leftrightarrow NO + N$	$O_2 + N \leftrightarrow NO + O$	Refs.
(39)	$\alpha = 0.51$	$\alpha = 0.24$	[48]
(40)	$\beta = 0$ $C = 4.17 \times 10^{12}$	$\beta = 1$ $C = 1.15 \times 10^{9}$	[49]
(41)	$\alpha = 0.52$ $\gamma = 0.90$	$\alpha = 0.12$ $\gamma = 0.46$	[51]

Table 2
The coefficients in Eq. (42).

Temperature, K	b_0	b_1	b_2	b_3
7000	10.99	7.809×10^{-1}	-6.605×10^{-2}	1.672×10^{-3}
10000	11.93	5.496×10^{-1}	-4.512×10^{-2}	1.257×10^{-3}
14000	12.58	3.919×10^{-1}	-2.978×10^{-2}	7.670×10^{-4}

Table 3
The coefficients in Eq. (43).

a_{00}	10.97	a_{10}	9.313×10^{-4}	a_{21}	4.651×10^{-9}
a_{01}	7.947×10^{-2}	a_{11}	-1.735×10^{-5}	a_{22}	1.252×10^{-9}
a_{02}	2.709×10^{-1}	a_{12}	-3.118×10^{-5}	a_{30}	8.162×10^{-12}
a_{03}	-7.159×10^{-2}	a_{13}	1.280×10^{-6}	a_{31}	-2.503×10^{-13}
a_{04}	1.052×10^{-2}	a_{20}	-1.268×10^{-7}	a_{40}	-1.964×10^{-16}

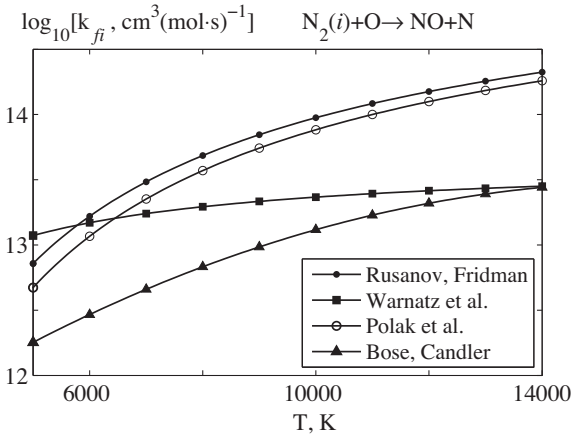

Fig. 1. The rate coefficients k_{fi} of reaction (37) as functions of temperature for $i = 10$.

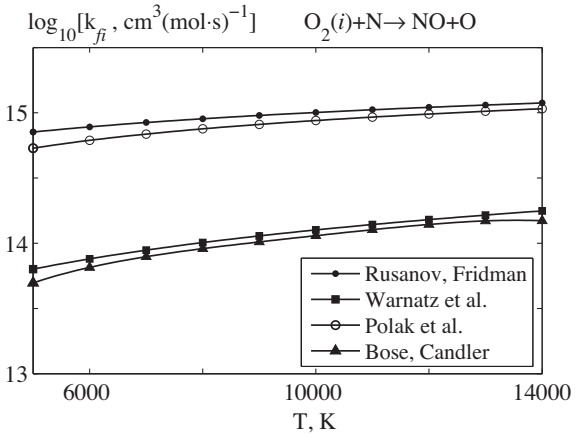

Fig. 2. The rate coefficients k_{fi} of reaction (38) as functions of the gas temperature for $i = 10$.

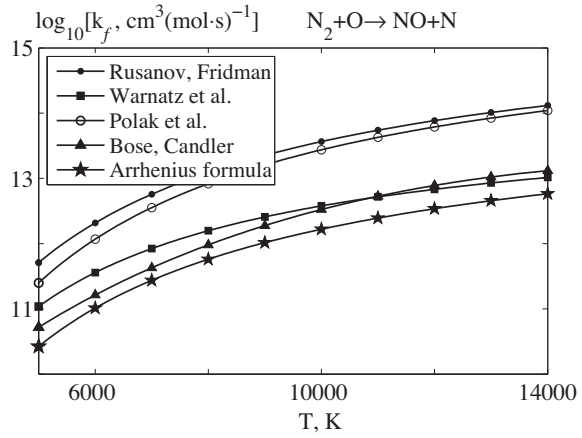

Fig. 3. The averaged rate coefficients k_f of reaction (37) as functions of temperature.

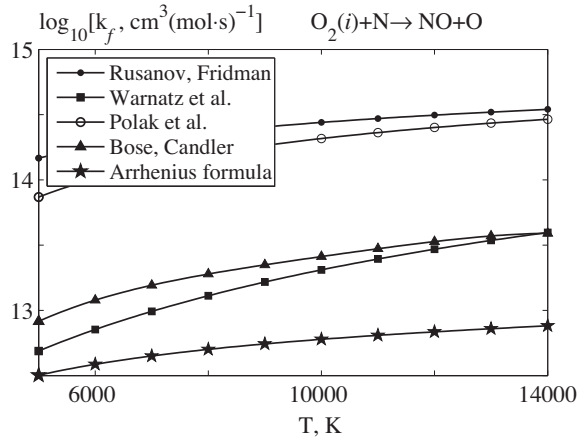

Fig. 4. The averaged rate coefficients k_f of reaction (38) as functions of temperature.

forward reaction whereas the rate coefficients for the forward reaction (38) exceed those for the backward reaction.

The expressions given above have been incorporated to the computational code for a solution of Eqs. (13)–(19). For the simplicity, in calculations only single-quantum VT, VV and VV' vibrational energy transitions are considered whereas multi-quantum jumps are neglected due to their lower probabilities. The effects of multi-quantum transitions at N_2–N collisions are discussed in [53,54]. Furthermore, it is supposed that NO molecules form in result of reactions (5) and (6) in the zero-th vibrational state and remain on this level during relaxation processes. In this case instead of 39 Eqs. (15) for NO vibrational level populations only one equation for the number density of NO molecules should be considered. This assumption is often accepted in calculations of different air flows [37,22,23,25] taking into account a small part of NO molecules in the air mixture under considered conditions. The influence of NO vibrational excitation on nozzle air flow parameters is shown in [25].

4. Results and discussion

4.1. The impact of free stream conditions and anharmonic effects on parameters behind a shock wave

In this section we report the results of numerical solution of Eqs. (13)–(19) for the following conditions in the free stream: $T_0 = 271$ K, $p_0 = 100$ Pa, $M_0 = 10, 15$, $n_{N_2}(0) = 0.79 n_0$, $n_{O_2}(0) = 0.21 n_0$,

$n_{NO}(0) = n_N(0) = n_O(0) = 0$ which correspond to the flight altitude $H = 48$ km.

Two cases of different vibrational level populations in the free stream are studied. In the first case, the vibrational distributions before a shock front are traditionally supposed to be thermal equilibrium with the temperature T_0 whereas in the second case we consider the shock wave appearing in the vibrationally excited air mixture. Such conditions may occur in the shock tube test section when the shock wave originates in a flow after its freezing in a nozzle (see for example [29]), in a flow near complex form bodies or in cases of another kinds of vibrational energy pumping before the shock front. In both considered cases the vibrational level populations just behind the shock front are the same as in the free stream because within the shock front they are assumed to be frozen due to substantial difference in relaxation times (see Eq. (1)). Macroscopic parameters just behind the shock front are connected with ones before the shock by conservation equations with frozen vibrational energies and mixture composition.

First, let us consider the relaxation zone structure in the case of the equilibrium vibrational distributions in the undisturbed flow, $M_0 = 15, 10$ and for Eq. (40) for the rate coefficients of the exchange reactions. The variation of the gas temperature and mixture composition is shown in Figs. 5–9. We can see a rapid decrease of the gas temperature and N_2, O_2 molar fractions close to the shock front due to dissociation and forward reactions (37), (38) and rising of number densities of atoms and NO molecules for $M_0 = 15$. Then accumulation of free atoms calls intensive reverse reaction (37) as well as reaction (38), which lead to non-monotonous n_{NO}/n changing for $M_0 = 15$. The low nitrogen atom concentration is explained by more intensive reaction (37) in the reverse direction and weak N_2 dissociation. For $M_0 = 10$ the vibrational activation and chemical relaxation proceed much slower because

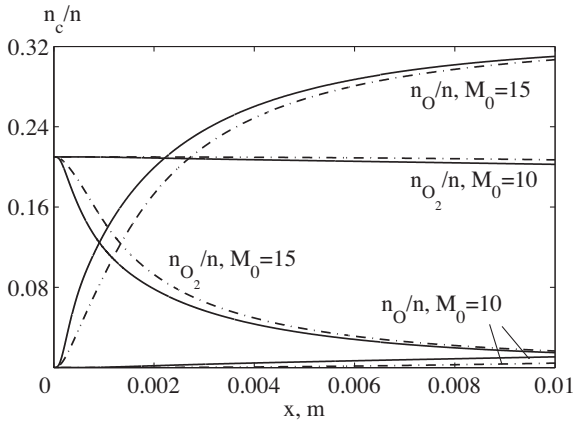

Fig. 7. The molar fractions n_{O_2}/n and n_O/n as functions of x. Solid and dash-dot curves correspond to anharmonic and harmonic oscillators, respectively.

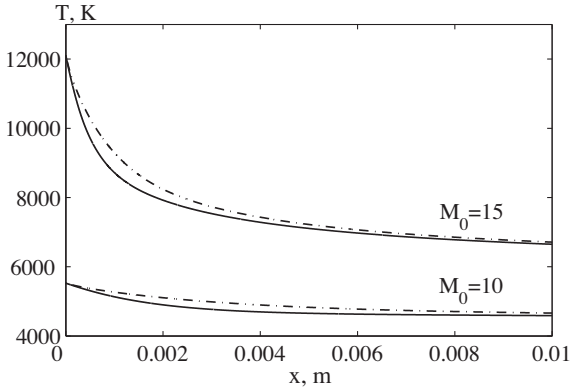

Fig. 5. The temperature T as a function of x. Solid and dash-dot curves correspond to anharmonic and harmonic oscillators, respectively.

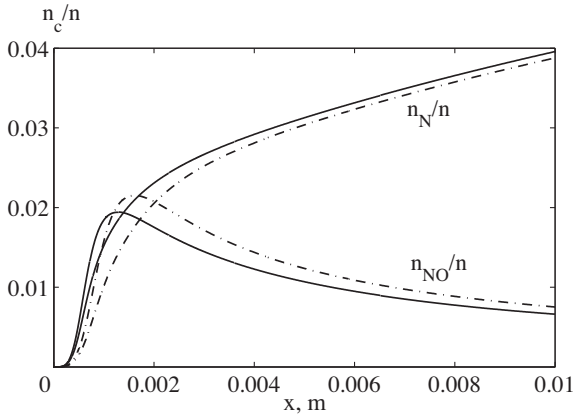

Fig. 8. The molar fractions n_{NO}/n and n_N/n as functions of x for $M_0 = 15$. Solid and dash-dot curves correspond to anharmonic and harmonic oscillators, respectively.

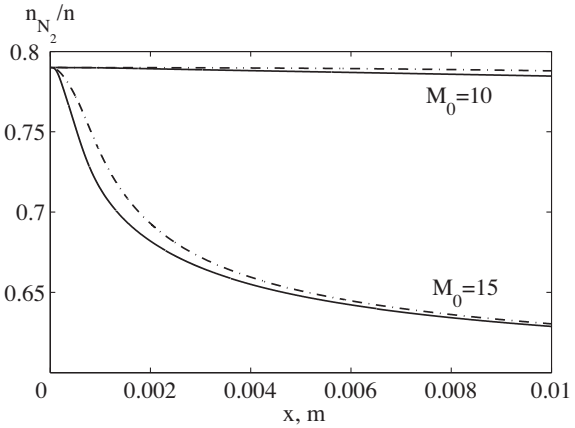

Fig. 6. The molar fraction n_{N_2}/n as a function of x. Solid and dash-dot curves correspond to anharmonic and harmonic oscillators, respectively.

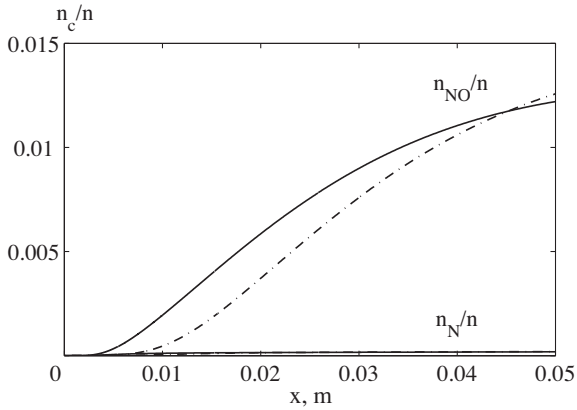

Fig. 9. The molar fractions n_{NO}/n and n_N/n as functions of x for $M_0 = 10$. Solid and dash-dot curves correspond to anharmonic and harmonic oscillators, respectively.

of lower temperature values just behind the shock front. Variation of n_{NO}/n in this case is shown in Fig. 9. Note that Fig. 9 is given on the extended scale because n_{NO} values in this case become much lower than for $M_0 = 15$.

Calculations show that neglecting anharmonic effects leads to overestimation of the gas temperature and N_2, O_2 molar fractions and underestimation of atomic number densities in the relaxation zone due to slower vibrational and chemical relaxation for harmonic oscillator. For $M_0 = 10$ this effect does not exceed 5% for the values T, n_{N_2} and n_{O_2}, while for $M_0 = 15$ it is more significant and consists about 6% for T and 17% for n_{O_2}.

Dimensionless (divided by n) N_2 and O_2 vibrational distributions for different distances from the shock front are presented in Figs. 10 and 11. In Table 4 the conditions corresponding to different lines in Figs. 10 and 11 are indicated. Table 5 presents vibrational energies of different levels of N_2 and O_2 molecules for harmonic and anharmonic oscillators. We would like to emphasize the non-monotonous variation of level populations with the distance from the shock front. First, they increase in result of the vibrational excitation of molecules (from the curve 1 for $x = 0$ to the curve 2 for $x = 5 \times 10^{-4}$ m in the case $M_0 = 15$) and then decrease (from the curve 2 towards to the curve 3 for $x = 10^{-2}$ m) due to vibrational energy transitions and chemical reactions. Note that the vibrational levels of N_2 molecules are populated less than those of O_2 molecules at the same distances from the shock front and their vibrational excitation proceeds slower. In the case $M_0 = 15$,

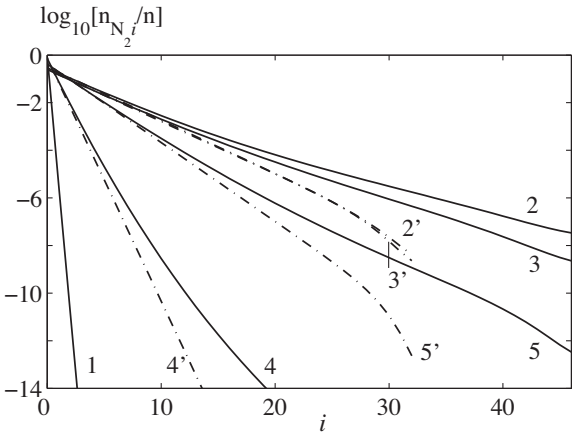

Fig. 10. The vibrational distributions $n_{N_2 i}/n$ for different values of x (see Table 4).

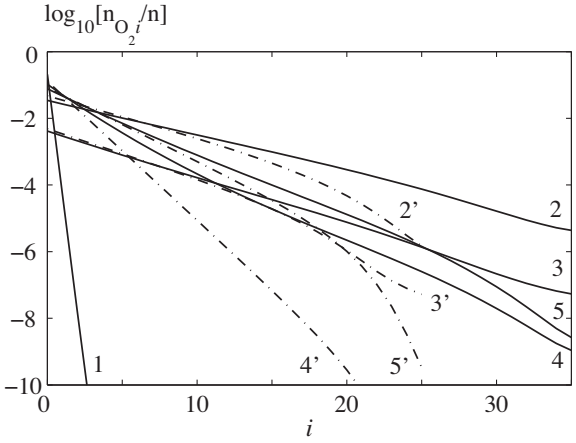

Fig. 11. The vibrational distributions $n_{O_2 i}/n$ for different values of x (see Table 4).

Table 4
Conditions corresponding to lines in Figs. 10 and 11.

		$x = 0$	$x = 5 \times 10^{-4}$ m	$x = 10^{-2}$ m
$M_0 = 15$	Anharmonic oscillator	Line 1	Line 2	Line 3
	Harmonic oscillator		Line 2′	Line 3′
$M_0 = 10$	Anharmonic oscillator	Line 1	Line 4	Line 5
	Harmonic oscillator		Line 4′	Line 5′

Table 5
Energies $\varepsilon_i^{N_2}$, $\varepsilon_i^{O_2}$ for different values of i for anharmonic and harmonic oscillator.

		$i = 5$	$i = 10$	$i = 15$	$i = 20$	$i = 25$	$i = 30$
$\varepsilon_i^{N_2}$, eV	Anhar. os.	1.55	2.87	4.09	5.23	6.29	7.25
	Har. os.	1.60	3.06	4.52	5.98	7.44	8.89
$\varepsilon_i^{O_2}$, eV	Anhar. os.	1.03	1.89	2.67	3.38	4.02	
	Har. os.	1.07	2.05	3.03	4.01	4.98	

the length of the zone of N_2 and O_2 vibrational excitation is found to be much shorter comparable to $M_0 = 10$. For $M_0 = 15$ it is about 0.08 cm for N_2 and 0.025 cm for O_2 or 12 and 4 mean free path lengths in the undisturbed flow, for $M_0 = 10$ these values increase in ten times.

The vibrational level populations of anharmonic oscillators (solid lines) noticeably exceed ones obtained for harmonic oscillators (dash-dot lines). This is compatible with the data given in [30] for (N_2, N) shock heated mixture and may be explained as an imposition of two effects. On the one hand, dissociation of anharmonic oscillators proceed faster than of harmonic oscillators, but on the other hand, the harmonic oscillator model yields underpopulated upper levels due to lower transition probabilities than for anharmonic oscillator.

Now, we consider the impact of vibrational excitation of molecules before the shock front on flow parameters behind a shock wave. The solution of the Eqs. (13)–(19) have been obtained with the vibrational level populations before the shock front taken in the form of non-equilibrium Boltzmann distributions with the vibrational temperatures $T_v^{N_2}$ and $T_v^{O_2}$ which are much higher than T_0. Two cases have been studied: $T_v^{N_2} = 2400$ K, $T_v^{O_2} = 1150$ K and $T_v^{N_2} = 8000$ K, $T_v^{O_2} = 4000$ K. The first case corresponds to the vibrational distributions in the freezing air flow in a parabolic nozzle with reservoir temperature $T = 8000$ K [22]. The second case specifies more strong initial excitation of molecules before the shock. Other conditions before the shock wave remain the same as given above for the equilibrium free stream.

Figs. 12 and 13 show the comparison of gas temperature, mixture composition and vibrational distributions obtained for the

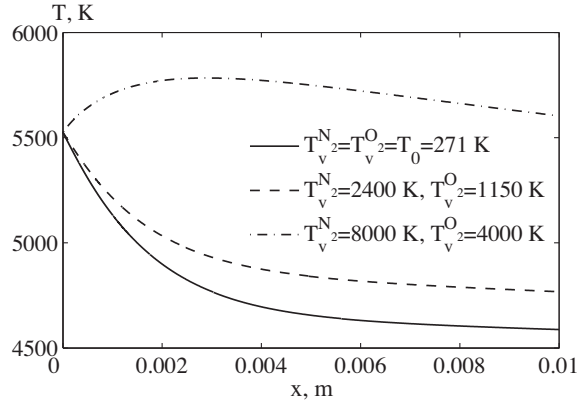

Fig. 12. The temperature T as a function of x, $M_0 = 10$.

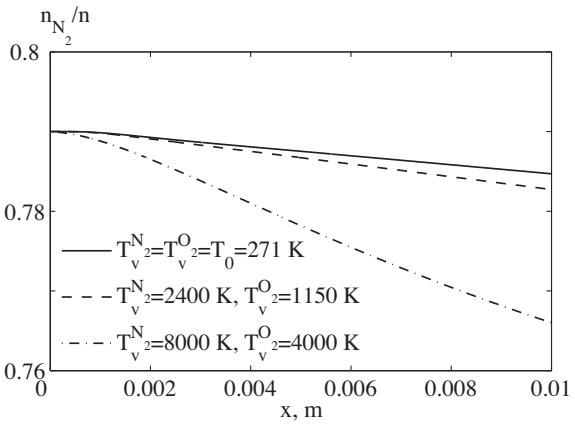

Fig. 13. The molar fraction n_{N_2}/n as a function of x, $M_0 = 10$.

cases of thermal equilibrium $\left(T_v^{N_2} = T_v^{O_2} = T_0\right)$ and non-equilibrium vibrational distributions before the shock front for $M_0 = 10$. In both cases of the initially non-equilibrium mixture, N_2 and O_2 molecules just behind the shock front occur already vibrationally excited. However, the principal difference exists between these cases: in the first case the vibrational temperatures remain lower than the value T_1 of the gas temperature immediately behind the shock ($T_1 > T_v^{N_2} > T_v^{O_2} > T_0$) whereas in the second case $T_v^{N_2}$ occurs higher than T_1 ($T_v^{N_2} > T_1 > T_v^{O_2} > T_0$). Results show that the relaxation zone structure changes dramatically in the second case. If $T_v^{N_2} > T_1$ the dominating process in a region close to the shock front is not *TV* vibrational excitation like in the previous cases of the equilibrium and weaker excited free stream, but deactivation due to *VT* vibrational energy transfer from highly excited N_2 molecules to the translational energy. In this case we can notice a non-monotonous variation of the gas temperature (Fig. 12) with the distance from the shock: first, T increases due to *VT* energy transitions and then it decreases in result of chemical reactions. Such a situation may appear behind shock waves with moderate Mach numbers generated in a strongly vibrationally excited gas. For the first case $T_1 > T_v^{N_2} > T_v^{O_2}$ further vibrational excitation of the flow proceeds faster than in the case of the equilibrium free stream $T_1 > T_v^{N_2} = T_v^{O_2} = T_0$ and the gas temperature in the relaxation zone in both cases occurs higher than for the vibrationally equilibrium free stream. It leads to more intensive dissociation and forward exchange reactions and, consequently, lower values of the molar fractions of molecules and higher values for atomic number densities (Fig. 13). The chemical relaxation proceeds much faster if $T_v^{N_2} > T_1$ and starts from the very beginning of the relaxation zone practically without a delay of N_2 dissociation and forward reaction (37) which takes place in the case of the equilibrium free stream.

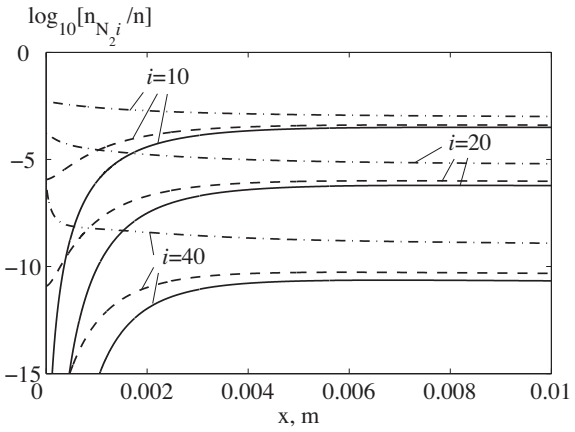

Fig. 14. The vibrational level populations $n_{N_2 i}/n$ as functions of $x, M_0 = 10$. Solid lines – $T_v^{N_2} = T_v^{O_2} = T_0 = 271$ K, dash lines – $T_v^{N_2} = 2400$ K, $T_v^{O_2} = 1150$ K, dash-dot lines - $T_v^{N_2} = 8000$ K, $T_v^{O_2} = 4000$ K.

Fig. 14 shows evolution of populations for several vibrational states of nitrogen molecules along the relaxation zone. The character of N_2 level populations variation is also quite different in the case $T_v^{N_2} > T_1$: populations of all the levels decrease just from the beginning of the relaxation zone due to *VT* their deactivation. For the equilibrium and weaker excited free stream level populations rise in the beginning of relaxation zone, this process proceeds more actively for the equilibrium flow before the shock wave.

We would like to emphasize a discrepancy between the limit temperature values for the thermally and chemically equilibrium mixture (in the end of the relaxation zone) in three considered cases. This is due to including of the initial vibrational energy to the total mixture enthalpy behind the shock front.

The influence of various non-equilibrium conditions before shock waves on shock heated flow parameters is a very interesting and important problem of the non-equilibrium gas dynamics which is still not completely studied particularly for multi-component mixtures with complicated kinetic processes. Some aspects of this problem and peculiarities of shock waves propagating in non-equilibrium gases are discussed in [55] (see also [33]).

4.2. The influence of the exchange reaction models on flow parameters in the relaxation zone

To study the influence of different models for exchange reactions on gas flow parameters and vibrational distributions in the relaxation zone we compare the results obtained with the use of four models for the rate coefficients of reactions (37) and (38) given in the Section 3. Figs. 15–18 present the results found for equilibrium vibrational distributions in the free stream and $M_0 = 15$.

Calculations show that the models of Rusanov, Fridman and Polak et al. provide very close values of the gas temperature (Fig. 15) and mixture composition (Fig. 16 for O_2 and O number densities), slightly deviating from the data given by the model of Warnatz et al., whereas the expressions proposed by Bose and Candler give the noticeable discrepancy in the values of these parameters. It is due to the fact that the latter equations do not take into account vibrational levels higher than $l_{N_2} = 30$ and $l_{O_2} = 15$, and therefore leads to lower values for the gas temperature and molar fractions of molecules and higher values for atomic number densities in comparison with other three models.

Comparison of populations of the vibrational levels $n_{N_2 i}/n$ for $i = 0, 20, 40$ and $n_{O_2 i}/n$ for $i = 0, 15, 30$ found on the basis of four

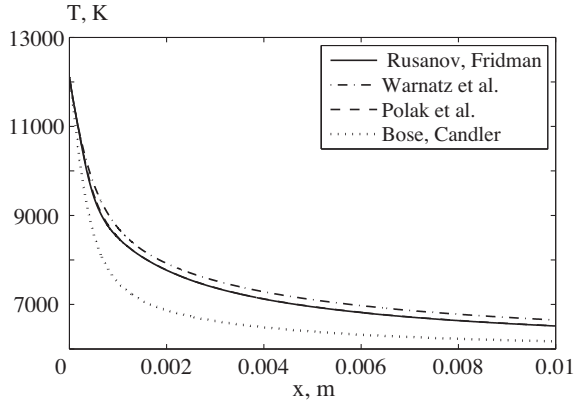

Fig. 15. The temperature T as a function of x, $M_0 = 15$.

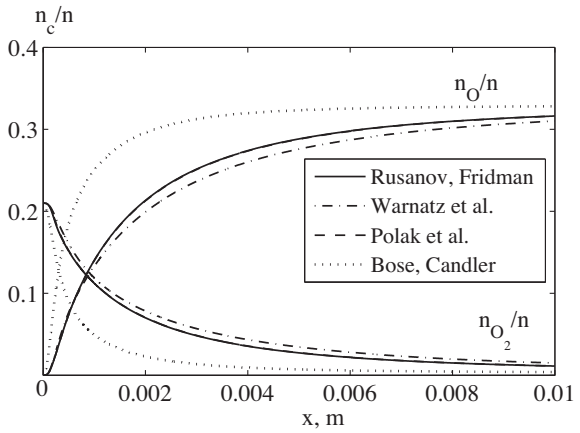

Fig. 16. The molar fractions n_{O_2}/n and n_O/n as functions of x, $M_0 = 15$.

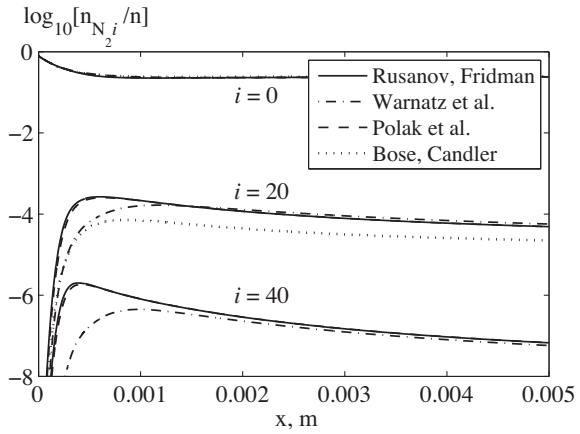

Fig. 17. The vibrational level populations $n_{N_2 i}/n$ as functions of x, $M_0 = 15$.

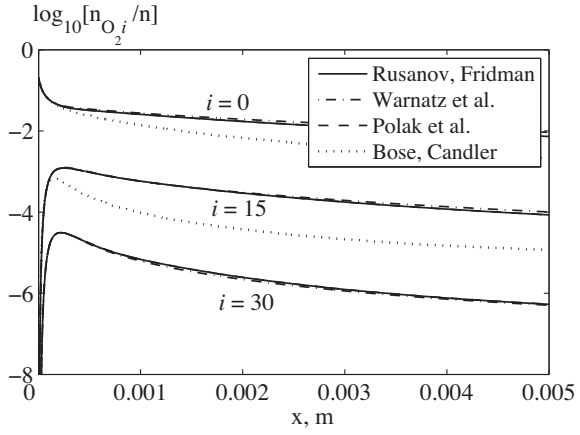

Fig. 18. The vibrational level populations $n_{O_2 i}/n$ as functions of x, $M_0 = 15$.

considered models is shown in Figs. 17 and 18. It reflects the character of the state-dependent rate coefficients for reactions (37) and (38) discussed in the Section 3. We can notice very close populations of low lying levels in the thin region close to the shock front, the difference becomes noticeable for higher levels. Then, with x rising, similarly to the number densities of molecular species, the models (39) and (41) give very close results, deviating slightly from the data obtained with the use of the expressions (40), whereas the expressions (42) and (43) provide more noticeable differences in the level populations.

4.3. Comparison of the state-to-state and simplified flow descriptions

Finally, we compare the results obtained in the state-to-state approximation with those found using the quasi-stationary two-temperature and one-temperature molecular distributions. Simplified models of vibrational-chemical kinetics make it possible to express distribution functions in terms of a few number of macroscopic parameters and, consequently, reduce a number of governing equations, therefore they are attractive for a practical use. Multi-temperature approaches for reacting mixtures are derived from the kinetic theory and applied for expanding and shock heated air flows in [32,56,3], recently reduced models for the state-to-state kinetics in hypersonic flows have been proposed in [57–59].

Comparison of the results obtained in the frame of simplified and accurate state-to-state flow descriptions provides an accuracy estimation for reduced approaches which is important in gas dynamic applications. We use two-temperature vibrational level populations in the form proposed by Treanor et al. [60] for a one-component gas of anharmonic oscillators with rapid *VV* exchanges and derived from the kinetic equations for distribution functions in reacting multi-component mixtures [3]:

$$n_{ci} = \frac{n_c}{Z_c^{vibr}(T, T_1^c)} \exp\left(-\frac{\varepsilon_i^c - i\varepsilon_1^c}{kT} - \frac{i\varepsilon_1^c}{kT_1^c}\right), \quad c = N_2, O_2, \tag{44}$$

where T_1^c is the temperature of the first vibrational level of species c, ε_1^c is its energy of the first level,

$$Z_c^{vibr}(T, T_1^c) = \sum_{i=0}^{l_c} \exp\left(-\frac{\varepsilon_i^c - i\varepsilon_1^c}{kT} - \frac{i\varepsilon_1^c}{kT_1^c}\right)$$

is the non-equilibrium vibrational partition function.

In this approach the set of macroscopic flow parameters in the considered mixture includes three temperatures T, $T_1^{N_2}$, $T_1^{O_2}$, velocity and number densities of all species. In this case 83 Eqs. (13) and (14) for level populations are reduced to four equations for n_{N_2}, n_{O_2} and temperatures $T_1^{N_2}$, $T_1^{O_2}$. Rate coefficients in these equations have been obtained by averaging of the state-dependent reaction rate coefficients over vibrational energies with distributions (44).

In the one-temperature approach $T_1^c = T$ and the expressions (44) are reduced to the Boltzmann equilibrium vibrational distributions with the gas temperature. In this case the governing equations for the considered mixture contain the equations for the macroscopic parameters n_{N_2}, n_{O_2}, n_{NO}, n_N, n_O, v, T and describe the flows of the thermal equilibrium reacting mixture.

The comparison of the gas temperature, number densities of oxygen molecules and atoms as well as the vibrational level populations for nitrogen molecules obtained in the state-to-state, three-temperature and one-temperature approaches is given in Figs. 19–21. The results are obtained for the following conditions $T_0 = 271$ K, $p_0 = 100$ Pa, $M_0 = 15$, and the equilibrium vibrational distributions in the free stream.

We can see that the simplified models noticeably underestimate (up to 20%) the gas temperature (Fig. 19) in the very beginning of the relaxation zone due to the assumption of the existence of quasi-stationary distributions just behind the shock front and do not describe the process of vibrational excitation.

Along with the temperatures $T_1^{N_2}$ and $T_1^{O_2}$ found in the frame of the three-temperature approximation, we calculated these values using the level populations obtained in the state-to-state approximation. Writing the equations (44) for $i = 1$ one can easy come to the expressions [36]:

$$T_1^{N_2} = \frac{\varepsilon_1^{N_2}}{k \ln\left(\frac{n_{N_2 0}}{n_{N_2 1}}\right)}, \quad T_1^{O_2} = \frac{\varepsilon_1^{O_2}}{k \ln\left(\frac{n_{O_2 0}}{n_{O_2 1}}\right)}, \tag{45}$$

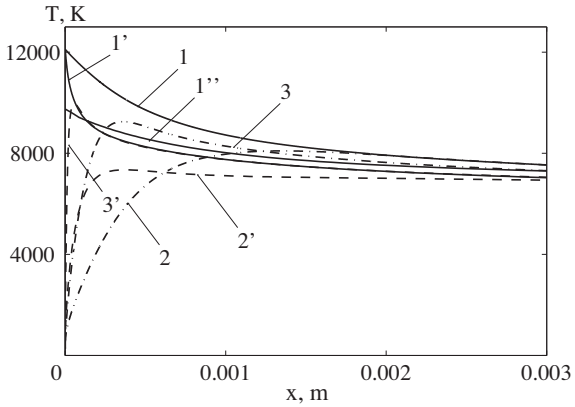

Fig. 19. The temperatures T, $T_1^{N_2}$ and $T_1^{O_2}$ as functions of x. The curves 1, 1′, 1″ correspond to T calculated in the state-to-state, three-temperature and one-temperature approaches, respectively; 2, 2′-$T_1^{N_2}$ and 3,3′-$T_1^{O_2}$ obtained in the state-to-state, three-temperature approaches, $M_0 = 15$.

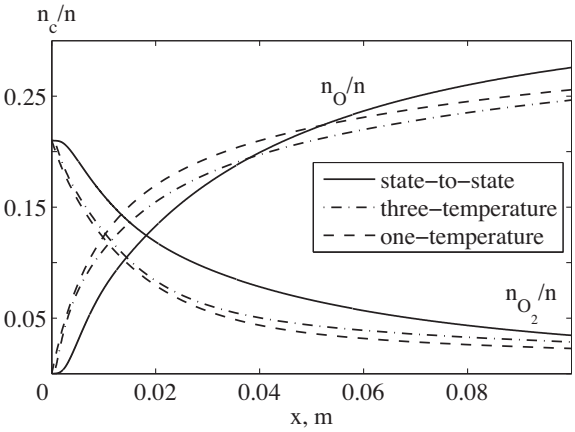

Fig. 20. The molar fractions n_{O_2}/n and n_O/n as functions of x, $M_0 = 15$.

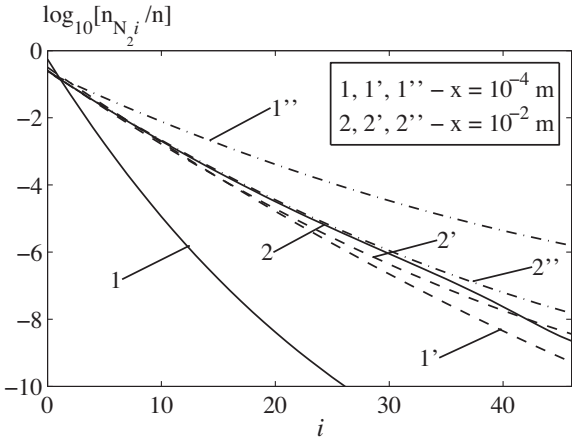

Fig. 21. The vibrational distributions $n_{N_2 i}/n$ for different values of x. 1, 2 – state-to-state approach; 1′, 2′ – three-temperature approach; 1″, 2″ – one-temperature approach, $M_0 = 15$.

where $n_{N_2 1}$, $n_{O_2 1}$ and $n_{N_2 0}$, $n_{O_2 0}$ are the level populations for $i = 1$ and $i = 0$ for N_2 and O_2 molecules found in the state-to-state approach.

One can notice that three-temperature model gives higher values of the temperatures $T_1^{N_2}$ and $T_1^{O_2}$ (discrepancy reaches 13%) than the expressions (45) with the level populations calculated with the use of the state-to-state approach, because of the same reason as mentioned above.

Quasi-stationary models overestimate the rates of variation of the number densities of atoms and molecules (see Fig. 20 for O_2 and O) and do not show the well known effect of a delay of free atoms formation in a thin layer near a shock which is found experimentally (see [13]) and is described in the detailed state-to-state calculations. Such a delay appears as a consequence of a lack of the vibrational energy of molecules for their dissociation in the beginning of the relaxation zone. Calculations show that overestimation of atomic number densities reaches 72% and 70% for the one-temperature and three-temperature models respectively, whereas maximum differences in molecular number densities do not exceed 34% and 22% for the one-temperature and three-temperature approaches.

Fig. 21 represents the vibrational distributions of nitrogen molecules in two positions behind the shock, found in the state-to-state, three-temperature and one-temperature approaches. The one-temperature approach greatly overestimates the vibrational level populations close to the shock front, the difference remains considerable for higher x values. The three-temperature approach shows distributions much closer to those obtained in the state-to-state approximation excluding a very thin region just behind the shock.

The discrepancy in macroscopic parameters obtained within three approaches reduces with the distance from the shock front rising and the mixture approaching the thermal and chemical equilibrium.

5. Conclusions

The paper presents the study of non-equilibrium flows of the five-component air mixture $N_2/O_2/NO/N/O$ behind shock waves on the basis of the detailed state-to-state description of vibrational and chemical kinetics. The vibrational energy transitions, dissociation, recombination and two Zeldovich reactions of NO formation are taken into account under the assumption of equilibrium distributions over velocities and rotational energies. The equations for populations of vibrational levels of molecular species and molar fractions of atoms are coupled to the momentum and total energy conservation equations and solved numerically for $M_0 = 10, 15$ in the free stream and different vibrational distributions before the shock front. The results show the strong influence of the free stream conditions on flow parameters and vibrational-chemical kinetics in the relaxation zone behind the shock wave. The considerable impact of the anharmonicity of molecular vibrations on the mixture composition and vibrational level populations is found. The neglect of anharmonicity effects leads to noticeable underestimation of populations of high lying levels and, correspondingly, lower dissociation and forward exchange reactions (37) and (38). The quite different structure of the relaxation zone is found for the cases of equilibrium and non-equilibrium vibrational distributions before the shock front. This effect is more pronounced for the case of high vibrational energy of molecules before the shock wave and moderate Mach numbers. Strong initial vibrational excitation leads to substantially more rapid chemical reactions and changes a character of the vibrational relaxation behind the shock wave.

In calculations four models of the state-dependent rate coefficients for Zeldovich exchange reactions presented in the literature are included to the numerical code and the influence of kinetic models on gas dynamic parameters, mixture composition and vibrational distributions in the relaxation zone is studied comparing the results obtained with the use of different models.

Along with the detailed state-to-state flow description, the simplified approach of vibrational-chemical kinetics based on the quasi-stationary multi-temperature vibrational distributions elaborated previously has been used in calculations. This approach is attractive for applications and considerably reduces the governing equations. The results are presented also for a thermal equilibrium one-temperature flow with non-equilibrium chemical reactions. The comparison of data found within two simplified approaches with those obtained in the accurate state-to-state approximation, made it possible to estimate the accuracy of the reduced models.

Conflict of interest

The authors declare that there are no conflicts of interest.

Acknowledgments

The authors acknowledge Saint-Petersburg State University for a research grant 6.38.73.2012. The work is partially supported by Grant No. 12-08-00826 of the Russian Foundation for Basic Research.

We are very grateful to Professor E. Kustova for useful discussions. We also grateful to I. Sharafutdinov for presented data obtained in the three-temperature and one-temperature approaches.

References

[1] V. Giovangigli, Multicomponent Flow Modeling, Springer, Berlin, 1999.
[2] R. Brun, Introduction to Reactive Gas Dynamics, Oxford University Press, 2009.
[3] E. Nagnibeda, E. Kustova, Nonequilibrium Reacting Gas Flows. Kinetic Theory of Transport and Relaxation Processes, Springer, Berlin, 2009.
[4] D. Bose, G.V. Candler, J. Chem. Phys. 104 (1996) 2825.
[5] D. Bose, G.V. Candler, J. Chem. Phys. 107 (1997) 6136.
[6] G. Chaban, R. Jaffe, D.W. Schwenke, W. Huo, Dissociation cross sections and rate coefficients for nitrogen from accurate theoretical calculations, in: 46th AIAA Aerospace Sciences Meeting and Exhibit, AIAA paper 2008-1209, January 2008.
[7] R. Jaffe, D. Schwenke, G. Chaban, Vibration–rotation excitation and dissociation in N_2–N_2 collisions from accurate theoretical calculations, in: 10th AIAA/ASME Joint Thermophysics and Heat Transfer Conference, AIAA Paper 2010-4517, June 2010.
[8] T.E. Magin, M. Panesi, A. Bourdon, R.L. Jaffe, D.W. Schwenke, Chem. Phys. 398 (2012) 90.
[9] A. Munafo, M. Panesi, R.L. Jaffe, G. Colonna, A. Bourdon, T.E. Magin, Eur. Phys. J. D 66 (7) (2012) 1.
[10] J.G. Kim, I.D. Boyd, Chem. Phys. 415 (2013) 237.
[11] M. Panesi, R.L. Jaffe, D.W. Schwenke, T.E. Magin, J. Chem. Phys. 138 (2013) 044312.
[12] A. Munafo, M. Panesi, T.E. Magin, Phys. Rev. E 89 (2014) 023001.
[13] Y. Stupochenko, S. Losev, A. Osipov, Relaxation in Shock Waves, Nauka, Moscow, 1965 (Engl. transl. Springer, Berlin, 1967).
[14] G. Chernyi, S. Losev, S. Macheret, B. Potapkin, Physical and Chemical Processes in Gas Dynamics, vols. 1–2, American Institute of Aeronautics and Astronautics, USA, 2004.
[15] L. Ibraguimova, O. Shatalov, High Temperature Phenomena in Shock Waves, Springer, Berlin, 2012, p. 99.
[16] E. Josyula, W.F. Bailey, J. Thermophys. Heat Transfer 15 (2) (2001) 157.
[17] E. Josyula, E. Kustova, P. Vedula, J.M. Burt, Influence of state-to-state transport coefficients on surface heat transfer in hypersonic flows, in: 52nd Aerospace Sciences Meeting, AIAA paper 2014-0864, January 2014.
[18] F. Lordet, J. Meolans, A. Chauvin, R. Brun, Shock Waves 4 (1995) 299.
[19] I. Adamovich, S. Macheret, J. Rich, C. Treanor, AIAA J. 33 (6) (1995) 1064.
[20] E. Kustova, E. Nagnibeda, The influence of the state-to-state distributions behind shock wave on the dissociation rates, in: Proceedings of the 22nd International Symposium on Shock Waves, vol. 1, 2000, pp. 783–788.
[21] B. Shizgal, F. Lordet, J. Chem. Phys. 104 (10) (1996) 3579.
[22] G. Colonna, M. Tuttafesta, M. Capitelli, D. Giordano, J. Thermophys. Heat Transfer 13 (3) (1999) 372.
[23] G. Colonna, M. Tuttafesta, M. Capitelli, D. Giordano, J. Thermophys. Heat Transfer 14 (3) (2000) 455.
[24] E. Kustova, E. Nagnibeda, T. Alexandrova, A. Chikhaoui, Chem. Phys. 276 (2) (2002) 139.
[25] S. Bazilevich, K. Sinitsyn, E. Nagnibeda, AIP Conf. Proc. 1084 (1) (2008) 843.
[26] I. Armenise, M. Capitelli, C. Gorse, J. Thermophys. Heat Transfer 10 (3) (1996) 397.
[27] I. Armenise, F. Esposito, M. Capitelli, Chem. Phys. 336 (2007) 83.
[28] G. Candler, J. Olejniczak, B. Harrold, Phys. Fluids 9 (7) (1997) 2108.
[29] C. Park, J. Thermophys. Heat Transfer 20 (4) (2006) 689.
[30] S. Losev, M. Pogosbekian, A. Sergievskaya, E. Kustova, E. Nagnibeda, AIP Conf. Proc. 762 (1) (2005) 1049.
[31] F. Esposito, M. Capitelli, E. Kustova, E. Nagnibeda, Chem. Phys. Lett. 330 (1) (2000) 207.
[32] A. Chikhaoui, J. Dudon, S. Genieys, E. Kustova, E. Nagnibeda, Phys. Fluids 12 (1) (2000) 220.
[33] M. Capitelli, C. Ferreira, B. Gordiets, A. Osipov, Plasma Kinetics in Atmospheric Gases, Springer Series on Atomic, Optical and Plasma Physics, vol. 31, Springer, Berlin, 2000.
[34] R. Brun (Ed.), High Temperature Phenomena in Shock Waves, Shock Wave Science and Technology Reference Library, vol. 7, Springer, Berlin, 2012.
[35] R. Schwartz, Z. Slawsky, K. Herzfeld, J. Chem. Phys. 20 (1952) 1591.
[36] B. Gordiets, A. Osipov, L. Shelepin, Kinetic Processes in Gases and Molecular Lasers, Nauka, Moscow, 1980 (Engl. transl. Gordon and Breach Science Publishers, Amsterdam, 1988).
[37] M. Capitelli, I. Armenise, C. Gorse, J. Thermophys. Heat Transfer 11 (4) (1997) 570.
[38] G.D. Billing, E.R. Fisher, Chem. Phys. 43 (3) (1979) 395.
[39] G.D. Billing, E.R. Kolesnick, Chem. Phys. Lett. 200 (4) (1992) 382.
[40] P.V. Marrone, C.E. Treanor, Phys. Fluids 6 (9) (1963) 1215.
[41] C. Park, Nonequilibrium Hypersonic Aerothermodynamics, J. Wiley and Sons, New York, Chichester, Brisbane, Toronto, Singapore, 1990.
[42] C. Park, J. Thermophys. Heat Transfer 7 (3) (1993) 385.
[43] F. Esposito, M. Capitelli, C. Gorse, Chem. Phys. 257 (2) (2000) 193.
[44] F. Esposito, M. Capitelli, Chem. Phys. Lett. 418 (4) (2006) 581.
[45] F. Esposito, I. Armenise, G. Capitta, M. Capitelli, Chem. Phys. 351 (1) (2008) 91.
[46] P. Gamallo, R. Martínez, R. Sayós, M. Gonzáles, J. Chem. Phys. 132 (2010) 144304.
[47] S. Akpinar, I. Armenise, P. Defazio, F. Esposito, P. Gamallo, C. Petrongolo, R. Sayós, Chem. Phys. 398 (2012) 81.
[48] V. Rusanov, A. Fridman, Physics of Chemically Active Plasma, Nauka, Moscow, 1984 (in Russian).
[49] J. Warnatz, U. Riedel, R. Schmidt, Advanced in Hypersonic Flows, Modeling Hypersonic Flows, Vol. 2, Birkhäuser, Boston, 1992.
[50] W. Gardiner, Combustion Chemistry, Springer, Berlin, 1984.
[51] L. Polak, M. Goldenberg, A. Levitskii, Numerical Methods in Chemical Kinetics, Nauka, Moscow, 1984 (in Russian).
[52] Test Case 2: Definition of shock tunnel testcases for gas radiation prediction in a planetary atmosphere, in: Proceedings of the International Workshop on Radiation of High Temperature Gases in Atmospheric Entry, Part II. Porquerolles, France (ESA SP-583, April 2004), p. 139.
[53] I. Armenise, M. Capitelli, R. Celiberto, G. Colonna, C. Gorse, A. Laganá, Chem. Phys. Lett. 227 (1) (1994) 157.
[54] E. Nagnibeda, K. Novikov, Vestnik of the St. Petersburg University: Mathematics, vol. 1, 2006, p. 91 (in Russian).
[55] A.I. Osipov, A.V. Uvarov, Phys. Usp. 35 (11) (1992) 903 (in Russian).
[56] A. Chikhaoui, E. Nagnibeda, E. Kustova, T. Alexandrova, Chem. Phys. 263 (2001) 111.
[57] G. Colonna, I. Armenise, D. Bruno, M. Capitelli, J. Thermophys. Heat Transfer 20 (3) (2006) 477.
[58] G. Colonna, L.D. Pietanza, M. Capitelli, J. Thermophys. Heat Transfer 22 (2008) 399.
[59] G. Colonna, L.D. Pietanza, M. Capitelli, AIP Conf. Proc. 1333 (1) (2011) 1365.
[60] C. Treanor, I. Rich, R. Rehm, J. Chem. Phys. 48 (1968) 1798.